

Scale invariance and viscosity of a two-dimensional Fermi gas

Enrico Vogt, Michael Feld, Bernd Fröhlich, Daniel Pertot, Marco Koschorreck,* and Michael Köhl
Cavendish Laboratory, University of Cambridge, JJ Thomson Avenue, Cambridge CB3 0HE, United Kingdom
 (Dated: March 22, 2019)

We investigate the collective excitations of a harmonically trapped two-dimensional Fermi gas from the collisionless (zero sound) to the hydrodynamic (first sound) regime. The breathing mode, which is sensitive to the equation of state, is observed at a frequency two times the dipole mode frequency for a large range of interaction strengths and temperatures, and the amplitude of the breathing mode is undamped. This provides evidence for a dynamical $SO(2,1)$ scaling symmetry of the two-dimensional Fermi gas. Moreover, we investigate the quadrupole mode to measure the shear viscosity of the two-dimensional gas and study its temperature dependence.

PACS numbers: 03.75.Ss 05.30.Fk 68.65.-k

Scale invariant behaviour plays an important role in many branches of physics. It is encountered both in fluctuations near critical points of phase transitions [1] and in particle physics when masses become unimportant at high energies [2]. In non-relativistic quantum mechanics, scale invariance implies that the Hamiltonian $H(x)$ scales under a dilatation of the spatial coordinate $x \rightarrow \lambda x$ according to $H(\lambda x) \rightarrow H(x)/\lambda^2$. This scaling symmetry allows one to make fundamental statements about thermodynamic properties. For example, even in a strongly interacting system in D dimensions, pressure P and energy density ϵ are related by the same simple equation of state $P = 2\epsilon/D$ as an ideal gas. One such system, which is of great interest in the ultracold atom, heavy-ion, and nuclear astrophysics communities, is the two-component Fermi gas in three dimensions interacting via a zero-range potential with a scattering length a_{3D} . At unitarity ($a_{3D} \rightarrow \infty$) it is scale- and conformally-invariant with universal properties [3–7]. For example, the equation of state at zero temperature becomes $\mu \propto E_F$, in which μ is the chemical potential and E_F is the Fermi energy, and the bulk viscosity ζ vanishes for arbitrary temperatures.

In two-dimensional systems scaling behaviour is more subtle. When the two-dimensional scattering length a_{2D} [8] approaches infinity, the gas becomes non-interacting. This implies that at zero temperature one finds $\mu = E_F \propto n_{2D}$ and hence the gas is trivially scale invariant. Here, n_{2D} is the density. At finite interaction strength, i.e., finite values of a_{2D} , the two-body scattering amplitude in two dimensions $f(q) = \frac{4\pi}{-\ln(q^2 a_{2D}^2) + i\pi}$ is momentum dependent. Evaluating $f(q)$ at a characteristic momentum, for example the Fermi wave vector k_F , leads to a density dependent coupling strength [9]. In a quantum field theoretical model of the superfluid Bose gas, it has been pointed out that this could give rise to a quantum anomaly that breaks scale invariance [10].

In the presence of an isotropic harmonic trap, the scale invariance of the homogeneous system is replaced by a dynamical $SO(2,1)$ scaling symmetry [11]. The $SO(2,1)$ group, or “Lorentz” group, is the group of ro-

tations in 2+1 dimensional space-time. For the trapped gas, the $SO(2,1)$ symmetry results in an excitation spectrum with modes spaced by exactly $2\omega_\perp$ [11, 12]. Here, ω_\perp denotes the trap frequency of the weakly confined axes. This generates a hydrodynamic breathing mode at a frequency $\omega_B = 2\omega_\perp$, independent of the interaction strength. Moreover, the mode frequency is independent of amplitude and the breathing mode should be undamped. However, the quantum anomaly resulting from the density-dependent coupling strength has been predicted to shift the hydrodynamic breathing mode by $\delta\omega_B/\omega_B \sim a_{3D}/l_z$ [10] where l_z denotes the extension of the gas in the strongly confined direction.

In this manuscript, we study an interacting two-dimensional Fermi gas using collective modes to investigate scale invariance and viscosity. We tune the ratio a_{3D}/l_z between -3 and 0 , which provides us with access to the hydrodynamic and the collisionless regimes. Previous experiments using ultracold atomic gases to study scale invariance of a two-dimensional Hamiltonian were limited to weakly interacting bosons in a regime where $0 < a_{3D}/l_z \ll 1$ [13, 14] and weakly interacting three-dimensional gases with a highly elongated symmetry [15].

In our experiment [16, 17], we create two-dimensional Fermi gases of ^{40}K atoms in a 50/50 mixture of the $|F = 9/2, m_F = -9/2\rangle$ and $|F = 9/2, m_F = -7/2\rangle$ states of the hyperfine ground state manifold. The Fermi gas is loaded into the standing wave potential of an optical lattice to create an array of two-dimensional gases. The trapping frequency along the strongly confined direction is $\omega_z = 2\pi \times 78 \text{ kHz}$ and the radial trapping frequency is $\omega_\perp = \sqrt{\omega_x \omega_y} \simeq 2\pi \times 125 \text{ Hz}$ with an anisotropy $\epsilon = |\omega_x - \omega_y|/2\omega_\perp$ below 2%. Along the axial direction we populate approximately 30 layers of the optical lattice potential with an inhomogeneous peak density distribution of typically 2×10^3 atoms per spin state per 2D gas at the center. We tune the interactions by applying a magnetic field close to the Feshbach resonance at 202.15 G [18].

First, we study the quadrupole mode of the two-dimensional Fermi gas in order to identify the collision-

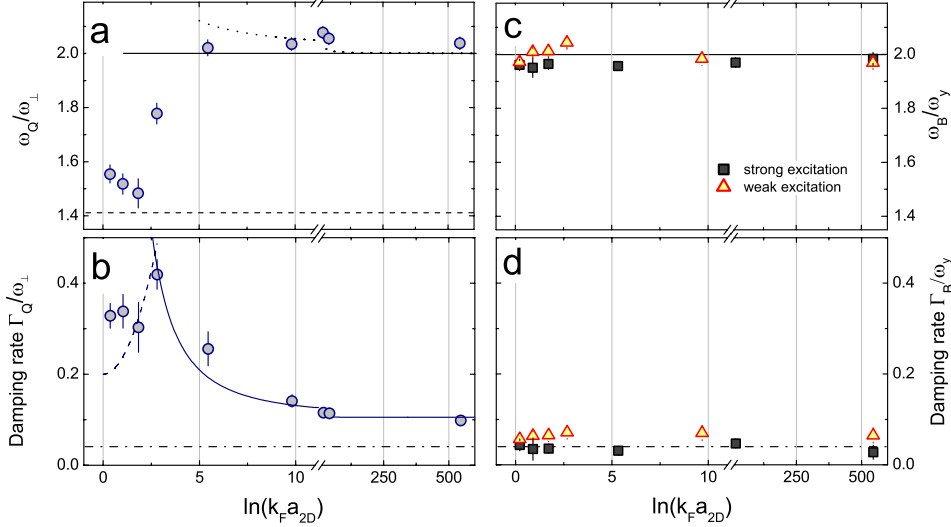


FIG. 1. (Color online) **a:** Frequency of the quadrupole mode at $T/T_F = 0.47$ with $E_F = \hbar \times (8.2 \pm 0.7)$ kHz. The dotted line shows the theoretical prediction of [19] in the collisionless limit and the dashed line at $\omega_Q/\omega_\perp = \sqrt{2}$ is the hydrodynamic mode. **b:** Damping of the quadrupole mode. The solid line shows the fits for Γ_0 and the dashed line for Γ_1 (see text). The dash-dotted line is the damping rate of the dipole mode. **c:** Frequency of the breathing mode. For the strong excitation we have $T/T_F = 0.37$ and $E_F = \hbar \times (5.4 \pm 0.8)$ kHz and for the weak excitation $T/T_F = 0.42$ and $E_F = \hbar \times (8.1 \pm 1.1)$ kHz. **d:** Damping of the breathing mode. The dash-dotted line is the damping rate of the dipole mode.

less and the hydrodynamic regimes. In the collisionless limit, surface modes are analogous to zero sound. At zero temperature the quadrupole mode frequency is predicted to be $\omega_Q = \sqrt{2(2 - \tilde{g})/(1 - \tilde{g})}\omega_\perp$ with $\tilde{g} = 1/\ln(k_F a_{2D})$ [19]. A collective hydrodynamic mode, in contrast, corresponds to a first sound mode. The frequency of the hydrodynamic quadrupole mode $\omega_Q = \sqrt{2}\omega_\perp$ [20, 21] is independent of the equation of state because its incompressible flow pattern prevents a change of the internal energy during the oscillation [22].

We excite the quadrupole mode by adiabatically introducing a small anisotropy to the two-dimensional harmonic oscillator potential using additional laser beams while maintaining $\omega_x \times \omega_y \approx \text{const.}$ and then abruptly returning to the original trapping configuration. The atomic cloud oscillates freely in this potential until we switch it off and take an absorption image after 12 ms of time of flight. The amplitude of the excitation after time-of-flight is 10% of the cloud size. We determine the radius of the cloud in the x- and the y-direction and fit their difference to measure ω_Q [23]. Owing to the change in gravitational sag during the excitation, we simultaneously excite small dipole (center-of-mass) oscillations primarily in the vertical y-direction. We use these dipole oscillations to calibrate $\omega_{x,y}$, of which ω_y has the smaller error because of the larger oscillation amplitude. The decay rate of the dipole mode $\Gamma_D/\omega_\perp = 0.04 \pm 0.01$ is most probably caused by the weak anharmonicity of our trapping potential.

In Figure 1a we show the quadrupole mode frequency ω_Q of the two-dimensional Fermi gas. For large values of the interaction parameter $\ln(k_F a_{2D})$ we are in the collisionless regime and observe $\omega_Q \simeq 2\omega_\perp$, in agreement with the theoretical expectation [19]. As we increase the interaction strength, i.e., decrease the value of $\ln(k_F a_{2D})$, we enter the hydrodynamic regime. This transition is marked by a sharp decrease of the collective

mode frequency to $\omega_Q \simeq \sqrt{2}\omega_\perp$. Theoretically, we expect the transition from the collisionless to the hydrodynamic regime when the collision rate γ_0 equals the mode frequency ω_Q . We estimate $\gamma_0 = -\hbar n_{2D} \text{Im}[f(k_F)]/m$ using the optical theorem for the scattering cross section $\sigma = -\text{Im}[f(q)]/q$. For very small deviations from the equilibrium distribution, the collision rate γ_0 is suppressed by a factor $(T/T_F)^2 < 1$ owing to the restriction of phase space because of Pauli's exclusion principle. Using our average density $n_{2D} \approx 6 \times 10^{12} \text{m}^{-2}$ and temperature $T/T_F = 0.47$ we estimate the transition from the hydrodynamic to the collisionless regime at an interaction parameter $\ln(k_F a_{2D}) \approx 3$, in good agreement with the observed mode frequency change.

In Figure 1b we show the damping rate Γ_Q of the quadrupole mode. The zero sound mode in the collisionless regime is damped by collisions which disrupt the coherent quasiparticle motion. Hence, the mode damping rate Γ_0 scales proportional to the normalized collision rate γ_0/ω_Q with an asymptotic behaviour $\Gamma_0 \propto [\ln(k_F a_{2D})]^{-2}$, shown as the solid line. The damping rate reaches a constant offset of $0.1\omega_\perp$, even for the non-interacting gas, which we will investigate in more detail below. For the first sound mode in the hydrodynamic regime the situation is opposite: collisions are necessary to establish local equilibrium and first sound is damped by the deviation from this, hence $\Gamma_1 \propto \omega_Q/\gamma_0$, which asymptotically is $\Gamma_1 \propto 1 + [2\ln(k_F a_{2D})/\pi]^2$ (dashed line). In the fit of the proportionality constant we have used the same constant offset as for the non-interacting gas. In between the two extremes, the damping rate peaks at the transition from the collisionless to the hydrodynamic regime.

Having identified the hydrodynamic and collisionless regimes, we now turn our attention to the breathing mode and the question of scale invariance of the two-

dimensional Fermi gas. The breathing mode is excited by adiabatically decreasing the strength of the two-dimensional confinement and then abruptly returning to the original trapping configuration. We identify the breathing mode frequency (Figure 1c) by studying the cloud radii in x - and y -direction as a function of hold time and define $\omega_B = \sqrt{\omega_{B,x}\omega_{B,y}}$. Again, we use the simultaneously excited dipole mode for continuous referencing. We study two sets of data of the breathing mode as a function of interaction strength which differ by a factor of 2 in excitation strength [24]. The weak excitation strength corresponds to 12% modulation of the width after time of flight. We observe that the mode frequency is approximately constant for all interaction strengths and averages at $\omega_B/\omega_y = 2.00 \pm 0.03$ for the weak excitation and at $\omega_B/\omega_y = 1.96 \pm 0.01$ for the strong excitation. We also have not observed any change of the mode frequency with the temperature of the gas in the range $0.37 < T/T_F < 0.9$.

The independence of the breathing mode frequency from interaction strength, oscillation amplitude, and temperature and the fact that the mode frequency is very close to $\omega_B = 2\omega_\perp$ suggest that the gas exhibits a dynamical $SO(2, 1)$ scaling symmetry. In the hydrodynamic normal regime, our result implies that the equation of state is polytropic and $\mu \propto n_{2D}$. Interestingly, this result is compatible with BCS mean field theory at finite temperature [21, 25]. A more precise determination of the equation of state, which also takes into account logarithmic interaction energy shifts and other beyond mean-field effects, could be obtained from Quantum-Monte Carlo calculations, which so far are only available for superfluids at zero temperature [26].

The damping of the breathing mode (Figure 1d) differs fundamentally from the quadrupole mode, because it is very small and independent of the interaction strength. In order to understand the undamped behaviour of the breathing mode, we employ a simplified model based on classical hydrodynamics. Energy dissipation of the velocity field $\mathbf{v}(\mathbf{r})$, and hence damping of the coherent motion of particles, is caused by the viscosity of the gas. The energy dissipation rate \dot{E} follows from the two-dimensional stress tensor [27] $\dot{E} = -\frac{1}{2} \int d^2r \eta(\mathbf{r})(\partial_k v_i + \partial_i v_k - \delta_{ik} \nabla \cdot \mathbf{v})^2 - \int d^2r \zeta(\mathbf{r})(\nabla \cdot \mathbf{v})^2$ with the shear viscosity $\eta(\mathbf{r})$ and the bulk viscosity $\zeta(\mathbf{r})$. The velocity field of the breathing mode has the form $\mathbf{v}(\mathbf{r}) = b[x\hat{\mathbf{e}}_x + y\hat{\mathbf{e}}_y] \cos(\omega t)$, with a constant b , and the time averaged energy dissipation rate is $\langle \dot{E} \rangle_t = -2b^2 \int d^2r \zeta(\mathbf{r})$, entirely determined by the bulk viscosity. The amplitude damping of the mode is $\Gamma = \langle \dot{E} \rangle_t / 2 \langle E \rangle_t$, using the total time-averaged kinetic energy $\langle E \rangle_t = \frac{mb^2}{4} \int d^2r r^2 n(\mathbf{r})$. In our data, the damping rate of the breathing mode averages near $\Gamma_B/\omega_y \simeq 0.05$, equal to the damping of the dipole mode which is dominated by technical limitations (e.g. dephasing due to trap anharmonicities) rather than by viscous forces. Additionally, we observe the absence of damping for differ-

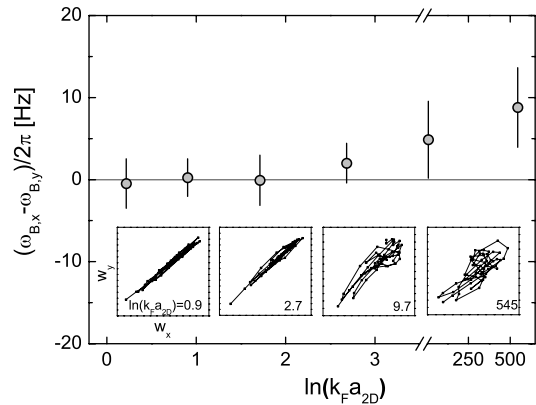


FIG. 2. Difference between the breathing mode frequencies of the two different axes at the collisionless-hydrodynamic crossover in a slightly anisotropic trap. The insets show the correlation plot of the cloud widths along the two axes.

ent excitation amplitudes and temperatures.

As a side remark, we observe the transition from the collisionless to the hydrodynamic regime also directly for the breathing mode. In a slightly anisotropic trap ($\epsilon < 0.02$) in the collisionless regime, the oscillation frequencies of the widths of the cloud are split by $2\epsilon\omega_B$, corresponding to two independent modes (see Figure 2). When the interaction strength is increased into the hydrodynamic regime the two mode frequencies lock together and the whole cloud undergoes a collective breathing mode at a single frequency. The occurrence of this “mode-locking” coincides with the values of $\ln(k_F a_{2D})$, where we observe the collisionless-hydrodynamic transition of the quadrupole mode. As insets we show correlation plots between the widths of the cloud demonstrating the change from nearly uncorrelated into highly correlated motion.

We now turn our attention to the temperature dependent damping of the quadrupole mode. The viscosity of a strongly interacting gas plays an important role in the investigation of the viscosity/entropy density ratio predicted by the AdS/CFT correspondence, which so far has been primarily investigated in three dimensions [28, 29]. In two dimensions, the shear viscosity of the Fermi gas and its temperature dependence have been theoretically investigated only in specific limits [30, 31], none of which correspond to our experimental situation. Our data for the temperature dependence of the damping rate Γ_Q are displayed in Figure 3a for various interaction strengths. We use the same model as above, which neglects possible temperature gradients as well as quantum statistics. For the quadrupole mode, the velocity field takes the form $\mathbf{v}(\mathbf{r}) = b[x\hat{\mathbf{e}}_x - y\hat{\mathbf{e}}_y] \cos(\omega t)$, with a constant b . The time averaged dissipation rate of the quadrupole mode is $\langle \dot{E} \rangle_t = -2b^2 \int d^2r \eta(\mathbf{r})$. Using the parametrization $\eta(\mathbf{r}) = \hbar n_{2D}(\mathbf{r}) \alpha(T/T_F)$ with a dimensionless function $\alpha(T/T_F)$ [7], we obtain $\alpha(T/T_F) = m \langle r^2 \rangle \Gamma_Q / 4\hbar$. We de-

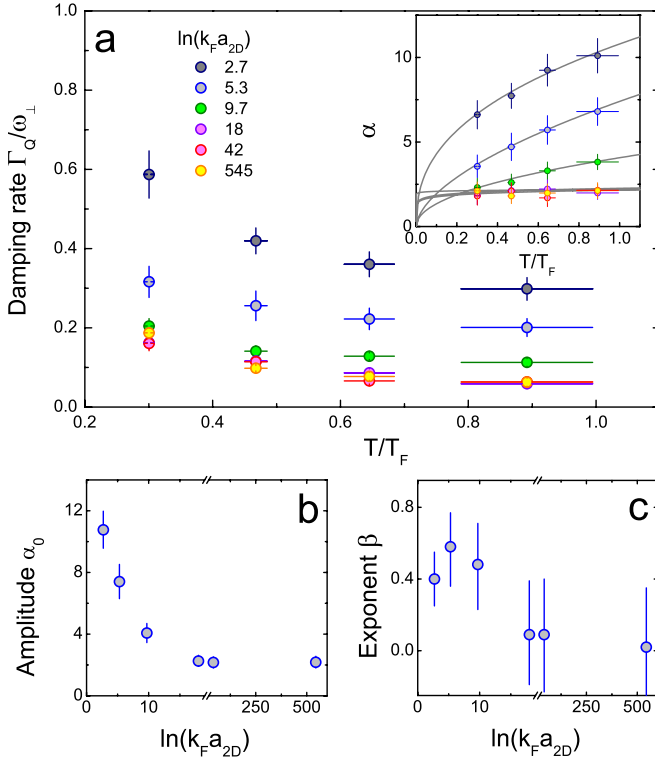


FIG. 3. (Color online) Temperature dependent damping of the quadrupole mode. **a**: Damping rate as a function of temperature for various interaction strengths. E_F/h for the data sets are (from lowest to highest temperature): 6.4 kHz, 8.2 kHz, 9.0 kHz, and 9.1 kHz. Inset: Derived values of $\alpha(T/T_F)$ and power-law fits. **b**: Viscosity amplitude α_0 . **c**: Power law exponent β .

termine the rms-radius of the cloud $\sqrt{\langle r^2 \rangle}$ numerically for the non-interacting gas. We fit our data with a power law $\alpha(T/T_F) = \alpha_0 \times (T/T_F)^\beta$, which is known to provide the high-temperature scaling in three dimensions. The extracted amplitudes α_0 and exponents β are shown in Figures 3b and 3c, respectively. In the collisionless regime we observe no significant temperature dependence (i.e. $\beta \simeq 0$) but a constant entropy density α , which at least in part could be due to technical limitations such as anharmonicities. In the interacting regime, the temperature dependence of the viscosity is significant with $\beta \simeq 1/2$. In contrast to three dimensions, where the viscosity has been investigated intensively [7, 28, 29], no theoretical prediction exists yet for this parameter range of a two-dimensional Fermi gas.

In conclusion, we have studied collective oscillations of a two-dimensional trapped Fermi gas in the collisionless and the hydrodynamic regimes. We have observed the existence of a breathing mode at two times the trap frequency, which is invariant against interaction strength, amplitude of the excitation, and temperature. Moreover, this breathing mode is undamped as compared to the dipole mode. These observations suggest a dy-

namic $SO(2,1)$ scaling symmetry of the trapped two-dimensional Fermi gas. In our parameter range we do not observe indications for a quantum anomaly breaking scale invariance. Using the quadrupole mode, we have additionally studied the temperature-dependence of the shear viscosity of the two-dimensional Fermi gas.

We thank Y. Castin, M. Olshanii, and W. Zwerger for discussions. The work has been supported by EPSRC (EP/G029547/1), Daimler-Benz Foundation (B.F.), Studienstiftung, and DAAD (M.F.).

* E-mail: mk673@cam.ac.uk

- [1] J. Zinn-Justin, *Quantum Field Theory and Critical Phenomena* (Oxford University Press, 1996).
- [2] S. Coleman, *Aspects of Symmetry* (Cambridge University Press, 1985).
- [3] K. O'Hara, S. Hemmer, M. Gehm, S. Granade, and J. Thomas, *Science* **298**, 2179 (2002).
- [4] T.-L. Ho, *Phys. Rev. Lett.* **92**, 090402 (Mar 2004).
- [5] D. T. Son, *Phys. Rev. Lett.* **98**, 020604 (2007).
- [6] Y. Nishida and D. T. Son, *Phys. Rev. D* **76**, 086004 (Oct 2007).
- [7] T. Enss, R. Haussmann, and W. Zwerger, *Annals of Physics* **326**, 770 (2011).
- [8] Following D. Petrov and G. Shlyapnikov, *Phys. Rev. A* **64**, 012706 (2001), we use the definition $E_B = \hbar^2/ma_{2D}^2$ in which E_B is the binding energy of the dimer state.
- [9] P. Bloom, *Phys. Rev. B* **12**, 125 (Jul 1975).
- [10] M. Olshanii, H. Perrin, and V. Lorent, *Phys. Rev. Lett.* **105**, 095302 (Aug 2010).
- [11] L. P. Pitaevskii and A. Rosch, *Phys. Rev. A* **55**, R853 (Feb 1997).
- [12] F. Werner and Y. Castin, *Phys. Rev. A* **74**, 053604 (2006).
- [13] C.-L. Hung, X. Zhang, N. Gemelke, and C. Chin, *Nature* **470**, 236 (2011).
- [14] T. Yefsah, R. Desbuquois, L. Chomaz, K. J. Günter, and J. Dalibard, *Phys. Rev. Lett.* **107**, 130401 (Sep 2011).
- [15] F. Chevy, V. Bretin, P. Rosenbusch, K. Madison, and J. Dalibard, *Phys. Rev. Lett.* **88**, 250402 (2002).
- [16] B. Fröhlich, M. Feld, E. Vogt, M. Koschorreck, W. Zwerger, and M. Köhl, *Phys. Rev. Lett.* **106**, 105301 (2011).
- [17] M. Feld, B. Fröhlich, E. Vogt, M. Koschorreck, and M. Köhl, *Nature*, in press; ArXiv:1110.2418(2011).
- [18] We use the Feshbach resonance parameters from N. Strohmaier *et al.*, *Phys. Rev. Lett.* **104**, 080401 (2010).
- [19] T. Ghosh and S. Sinha, *Eur. Phys. J. D* **19**, 371 (2002).
- [20] W. Wen and G. Huang, *Phys. Lett. A* **362**, 331 (2007).
- [21] S. N. Klimin, J. Tempere, J. T. Devreese, and B. Van Schaeybroeck, *Phys. Rev. A* **83**, 063636 (2011).
- [22] A. Bulgac and G. F. Bertsch, *Phys. Rev. Lett.* **94**, 070401 (Feb 2005).
- [23] A. Altmeyer, S. Riedl, M. J. Wright, C. Kohstall, J. H. Denschlag, and R. Grimm, *Phys. Rev. A* **76**, 033610 (2007).
- [24] For the weak excitation of the breathing mode the spin imbalance was 10% and the data point at $\ln(k_F a_{2D}) = 2.7$ has $\epsilon = 4.1\%$.
- [25] V. M. Loktev, R. M. Quick, and S. Sharapov, *Physics*

- Reports **349**, 1 (2001).
- [26] G. Bertaina and S. Giorgini, Phys. Rev. Lett. **106**, 110403 (2011).
- [27] L. Landau and E. Lifshitz, *Fluid Mechanics*, Vol. 6 (Butterworth-Heinemann, 1976).
- [28] P. Kovtun, D. Son, and A. Starinets, Phys. Rev. Lett. **94**, 111601 (Mar 2005).
- [29] C. Cao, E. Elliott, J. Joseph, H. Wu, J. Petricka, T. Schäfer, and J. E. Thomas, Science **331**, 58 (2011).
- [30] D. S. Novikov, arXiv:cond-mat/0603184v1(2006).
- [31] J. Hofmann, arXiv:1106.6035v1(2011).